Bioorganic & Medicinal Chemistry 20 (2012) 5941–5947

Contents lists available at SciVerse ScienceDirect

Bioorganic & Medicinal Chemistry

journal homepage: www.elsevier.com/locate/bmc

# Development of a bifunctional chelating agent containing isothiocyanate residue for one step F-18 labeling of peptides and application for RGD labeling

Dinesh Shetty, Jae Min Jeong *, Young Ju Kim, Ji Youn Lee, Lathika Hoigebazar, Yun-Sang Lee, Dong Soo Lee, June-Key Chung

*Department of Nuclear Medicine, Department of Radiation Applied Life Science and Institute of Radiation Medicine, Seoul National University College of Medicine, Seoul, Republic of Korea*
*Clinical Research Institute and Cancer Research Institute, Seoul National University Hospital, Seoul, Republic of Korea*

ARTICLE INFO

*Article history:*
Received 28 May 2012
Revised 21 July 2012
Accepted 23 July 2012
Available online 7 August 2012

*Keywords:*
NODA
Al$^{18}$F
NO2A
c(RGDyK)
Angiogenesis imaging
Bifunctional chelating agent
Aluminum fluoride

ABSTRACT

We report herein a novel isothiocyanate active ligand for fluorine-18 labeling prepared by four step synthesis. It can be conjugated to a target molecule containing an amino functional group under weak basic conditions by way of thiourea bond formation. We explored the application of synthesized ligand by conjugating to well known $\alpha_v\beta_3$ integrin targeting peptide, c(RGDyK). The conjugated peptide showed good radiochemical yield and efficiency with an excellent radiochemical purity (97.1 ± 1.2%) in a short reaction time (10 min). Labeled peptide showed excellent in vitro and in vivo stability (>95%). $\alpha_v\beta_3$ integrin specific tumor uptake was observed both in biodistribution and small animal microPET studies on $\alpha_v\beta_3$-positive U87MG (human glioma cells) xenograft bearing mice. In general, successful application of synthesized ligand for labeling of RGD peptide could facilitate the possibility of using this ligand for labeling peptides containing an amino functional group.



## 1. Introduction

$^{18}$F-labeling of peptides has usually been performed in a multi-step process by first labeling a suitable synthon and conjugating it to the peptide via formation of amide, oxime, hydrazone, or by using thiol reactive maleimide synthons.[1–5] However, all these methods require additional steps that include purification of radiolabeled synthons before conjugation and final products should be re-purified to achieve high specific activity and purity as well as to remove organic solvent.

A novel method for the one step $^{18}$F-labeling of peptides using [$^{18}$F]AlF (aluminum fluoride) complex formation with 1,4,7-triazacyclononane-1,4,7-triacetic acid (NOTA) derivatives has been reported, which did not need a drying step neither before nor after the labeling.[6,7] For radiofluorination strategies involving NOTA-AlF chelation chemistry, the labeling procedure can be accomplished in water. From a biological perspective, these one-step and water-compatible reactions are ideal for incorporation of [$^{18}$F]fluoride into biomolecules. Although, NOTA has been proved to be an efficient chelating agent for labeling with $^{68}$Ga,[8–11] it was not so for [$^{18}$F]AlF method. Recently, significant increase of [$^{18}$F]AlF labeling efficiency was reported if 1,4,7-triazacyclononane-1,4-diiacetic acid (NODA) with a benzyl group attached to one of the nitrogen atoms of the cylcononane ring.[12–16] Another successful report of [$^{18}$F]AlF labeling application was NODA-nitroimidazole conjugates for hypoxia imaging.[17] To apply these processes into labeling of biomolecules, we designed a novel bifunctional chelating agent that has an active conjugation site for an amino group. Herein, we report an isothiocyanatobenzyl NODA (NODA-Bz-SCN, **5**) derivative that can be conjugated to biomolecules under mild conditions.

Integrins play important roles in the regulation of cellular activation, migration, proliferation, survival, and differentiation.[18,19] In particular, angiogenesis factor $\alpha_v\beta_3$ integrin is important for growth of various cancers.[20–22] Therefore, imaging $\alpha_v\beta_3$ integrin expression in tumors is important for staging cancer and for the patient's selection of anti-integrin treatments. Integrins represent a subclass of cell adhesion molecules connecting the cytoskeleton with the extracellular matrix (ECM) or other cells with the exposed RGD tripeptide sequence.[23–25] Integrin $\alpha_v\beta_3$ is highly expressed on activated endothelial cells but not quiescent endothelial cells of established vessels,[26] making it a suitable target for anti-angiogenic cancer management. After introduction of $\alpha_v\beta_3$ selective RGD peptides,[23,24] a variety of RGD based probes have been developed for PET imaging of $\alpha_v\beta_3$ integrin.[27–30] Thus, RGD probes have been used in clinical trials such as [$^{18}$F]galacto-RGD and [$^{18}$F]AH111585,

* Corresponding author. Tel.: +82 2 2072 3805; fax: +82 2 745 7690.
*E-mail address:* jmjng@snu.ac.kr (J.M. Jeong).

0968-0896/$ - see front matter © 2012 Elsevier Ltd. All rights reserved.
http://dx.doi.org/10.1016/j.bmc.2012.07.050

which require multistep procedures for $^{18}$F-labeling. The former requires four chemical reactions and three radio high performance liquid chromatography (radio-HPLC) purification steps,[31–33] and the latter requires two chemical reactions and two HPLC purification steps.[34–36] Due to the short half-life of $^{18}$F, repeated purification steps can be critical to obtain a higher yield and a more reliable method is required. Thus we synthesized **5**, conjugated it with a arginine–glycine–aspartic (RGD) peptide and studied its biological activities to confirm the applicability of this agent.

## 2. Results and discussion

### 2.1. Chemistry

The synthetic pathway of **5** is depicted in Scheme 1. The synthesis began with formation of **1** from cyclononane according to a previously reported method.[16] Nucleophilic substitution of **1** with 4-nitrobenzylbromide resulted in **2**, which was purified by column chromatography. *Tert*-butyl protection was removed by acid hydrolysis to yield **3**. Successive catalytic hydrogenation of **3** under basic condition produced **4** which were purified by prep-HPLC. Basic condition was crucial to avoid cleavage of benzyl carbon and cyclononane nitrogen bonds. The amino group was converted into isothiocyanate using thioposhgene in the solvents mixture. The final product **5** was purified by prep-HPLC and obtained as a fine solid. Easy handling and high stability of this agent at room temperature enhance the possibility of general application for biomolecule conjugation. It is a common knowledge that reactive isothiocyanate groups can be easily conjugated to amino groups of biomolecules under mild basic conditions in aqueous buffer. The high water solubility of the synthesized ligand was adequate for conjugating with peptide or protein molecules.

In the present study, we conjugated **5** with c(RGDyK) peptide to test the labeling efficiency and feasibility for angiogenesis imaging (Scheme 2). The extended amino group of lysine in the peptide was conjugated with **5** in the buffer solution (pH ~9) with quantitative yield. Conjugated product **6** was purified by prep-HPLC and was eluted at 9.6 min without any other peaks (see Supplementary Fig. 1).

### 2.2. Radiochemistry

To conduct the labeling, [$^{18}$F]fluoride was prepared as previously described,[37] and [$^{18}$F]$AlF^{2+}$ was prepared by mixing $Al^{3+}$ (45 nmol) with [$^{18}$F]fluoride (370 MBq) in 50 μL saline solution at room temperature for 10 min. The ligand conjugated peptide, **6** (50 nmol), was mixed with the prepared [$^{18}$F]$AlF^{2+}$ solution, and reactions were monitored at 95–110 °C after 10 min. Labeling efficiencies were determined using Instant Thin Layer Chromatography–Silica Gel (ITLC–SG) and labeled peptide was purified by radio-HPLC (Fig. 1). We succeeded in purifying the labeled peptide using HPLC or a C-18 cartridge but failed using an Alumina-N Cartridge (Fig. 2). The final radiochemical purity obtained was 97.1 ± 1.2% and the labeling efficiency was 57.9 ± 8.8%. The time for whole labeling and purification procedure was less than 25 min. [$^{18}$F]**7** demonstrated higher stability than 95% for 4 h in the prepared medium at room temperature and in human serum at 37°C by ITLC–SG analysis (see Supplementary Fig. 2).

### 2.3. In vivo studies

Biodistribution experiment was performed in U87MG tumor-bearing nude mice at 1 h after tail vein injection of [$^{18}$F]**7**. Blocking study was performed after injection of c(RGDyK) (3 mg/kg). The results are shown in Fig. 3. The tumor uptake of [$^{18}$F]**7** was 4.41 ± 0.98% ID/g. The uptake values in the other major organs except kidney were significantly lower than tumor uptake. High uptakes in the kidneys and liver indicate tracer excretion via both the renal and hepatobiliary routes. The tumor to muscle and the tumor to blood ratios were 8.17 ± 0.50 and 4.95 ± 0.36% ID/g, respectively. Low bone uptakes demonstrated in vivo stability of the agent. In the blocking study, a decrease of radioactivity was observed in all the organs, but it was most significant with tumor uptake, which was reduced markedly from 4.41 ± 0.98 to 1.33 ± 0.20% ID/g at 1 h post-injection ($p$ = 0.00083)

The in vivo tumor targeting property of [$^{18}$F]**7** was evaluated in U87MG tumor-bearing nude mice using dynamic small animal microPET scans at 1 and 2 h post injection (Fig. 4A). Tumor uptake was observed clearly at 1 and 2 h after injection but it decreased by time. High bladder uptake demonstrated that the tracer was rapidly excreted via the renal system, and low soft tissue uptakes were observed. The decreased tumor uptakes after blocking c(RGDyK) (3 mg/kg) confirmed the integrin $\alpha_v\beta_3$-specific targeting of the labeled agent. For quantitative analysis of imaging data, we calculated standardized uptake value (SUV), which is defined as a ratio of tissue radioactivity concentration (MBq/mL) at time t and injected dose (MBq) at the time of injection divided by body weight (g) in PET image. [$^{18}$F]**7** demonstrated tumor SUV of 7.42 ± 0.49 and

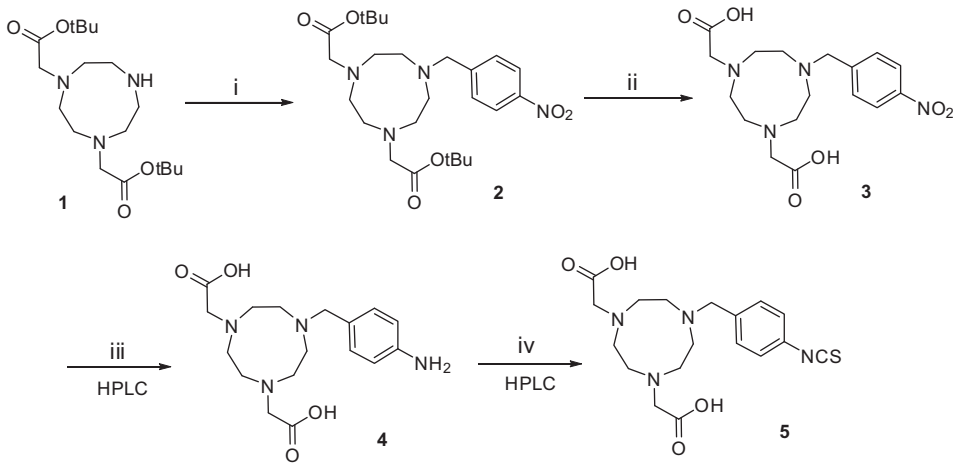


**Scheme 1.** Synthetic pathway for the formation of NODA-SCN Chelator (5). (i) 4-nitro benzyl bromide, $K_2CO_3$, ACN, rt; (ii) 4 M HCl in dioxane, rt; (iii) Pd–C, 2 mM KOH in MeOH, $H_2$, rt; (iv) $CSCl_2$, $CaCO_3$, $H_2O/CHCl_3$, rt.

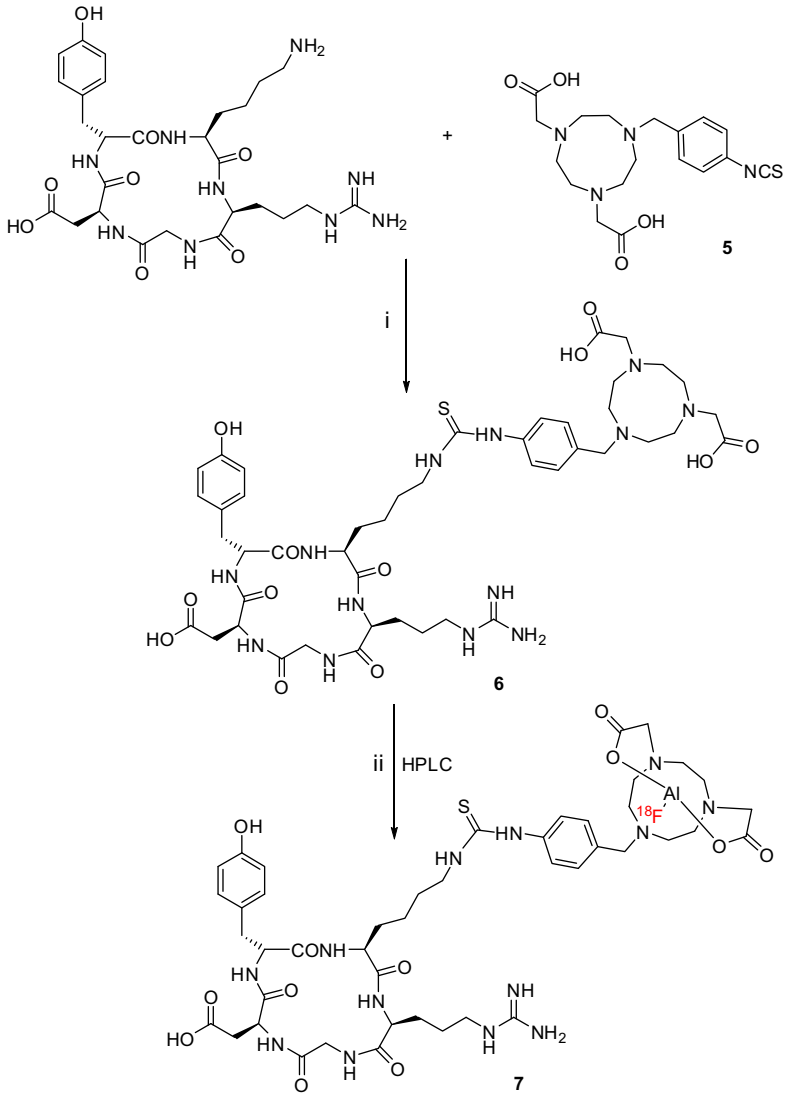


**Scheme 2.** Synthetic pathway for the formation of NODA-SCN-RGD (6) and Al$^{18}$F-NODA-SCN-RGD (7). (i) $Na_2CO_3$ buffer, pH 9, rt; (ii) $(Al^{18}F)^{2+}$, NaOAc buffer, pH 4, 110 °C, 10 min.

3.77 ± 0.57 at 1 and 2 h post injection, respectively, which decreased to 0.72 ± 0.14 and 0.42 ± 0.15, respectively, after blocking (Fig. 4B).

## 2.4. Discussion

The application of $^{18}$F-labeled RGD peptides for PET imaging of tumor angiogenesis increased rapidly. However, most established $^{18}$F-labeling procedures require multiple drying steps to obtain active [$^{18}$F]fluoride and are time consuming and make automation of the procedure difficult. Moreover, the reactions are usually performed in organic solvents which should be removed for clinical application. Therefore a straightforward single-step labeling strategy to obtain radiofluorinated RGD peptides is a clinical requirement. With the emergence of the [$^{18}$F]AlF labeling method, in which water is used as a reaction solvent, drying steps could be avoided. We tried to expand these findings for general $^{18}$F-labeling.[16,17] Interestingly, parallel works were reported recently on $^{18}$F labeled RGD dimers conjugated with NOTA that showed a similar trend in biodistribution and PET imaging studies.[38,39] Though our findings are unique due to general ligand synthesis for biomolecule conjugation, it might be necessary to compare those findings with present works, as researchers always tend to compare pharmacokinetics properties of labeled RGD monomers with dimers. Both in biodistribution and PET imaging studies, [$^{18}$F]**7** showed similar trend in tumor uptake and tumor to muscle ratio compared to RGD dimer. Notably, however, the reported works could achieve less than 25% radiochemical yield in the case of the RGD dimer, which is lower than the values we obtained with our ligand (57.9%). This difference of labeling yield is anticipated according to recent literature.[16] They used NOTA as a bifunctional chelating agent, which has an interfering carbonyl oxygen atom for $^{18}$F binding with aluminum, but our ligand NODA-Bz-SCN does not have such an interfering atom. Isothiocyanatobenzyl residue has been applied for easy conjugation of ligands with peptides or proteins containing amino groups. It is relatively stable compared to other amine conjugating agents, such as activated esters, and showed high conjugation yield. The formed thiourea bond is resistant to most hydrolyzing enzymes in the biological system.

## 3. Conclusion

NODA-Bz-SCN was synthesized as a bifunctional chelating agent for conjugation with peptide and labeling with $^{18}$F by a

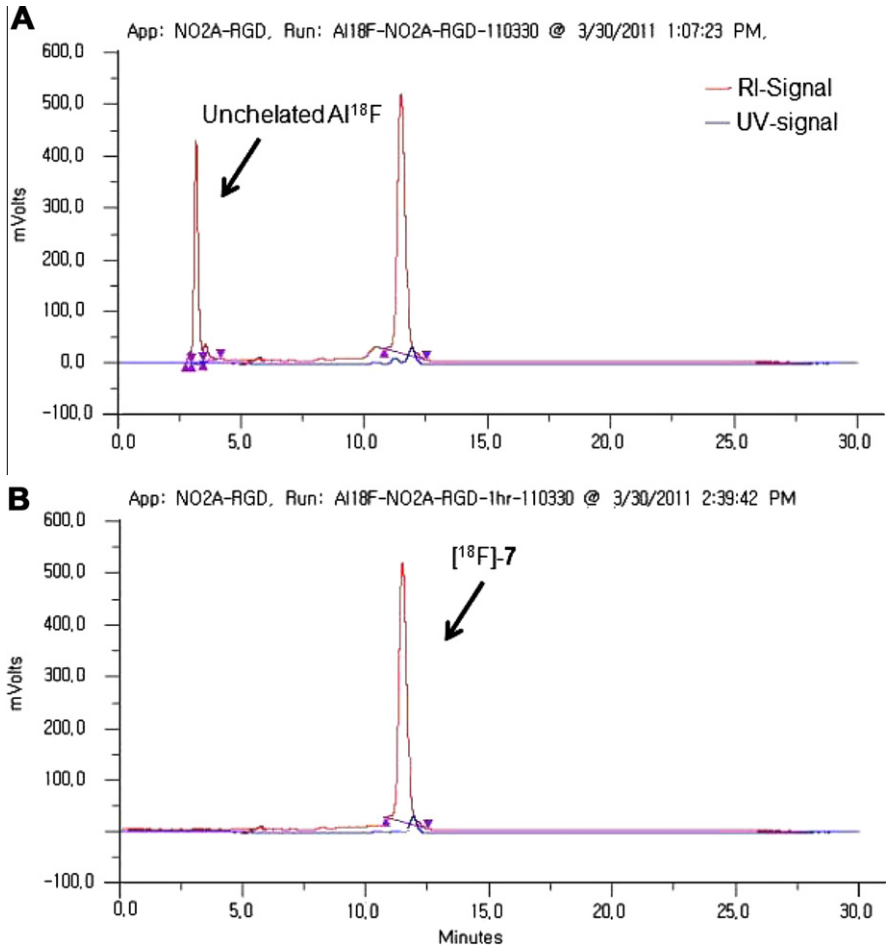


**Figure 1.** HPLC profile of radiotracer [$^{18}$F]7 before purification (A) and after purification (B). Samples were run on X-terra® 3.5 μm RP18 (4.6 × 100 mm) column; EtOH/0.05% TFA in water for 30 min with a flow rate of 1.0 mL/min; $t_R$ = 11.2 min.

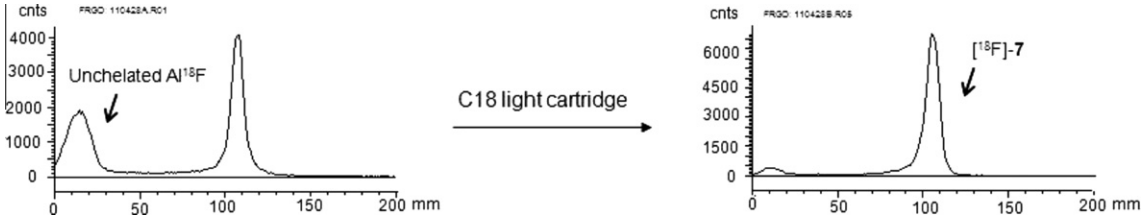


**Figure 2.** Purification of [$^{18}$F]7 using a C-18 cartridge. The reaction mixture was passed through the cartridge, washed with 10 mL distilled water and eluted with 1 mL EtOH.

chelating method, and it was successfully conjugated to RGD peptide. The conjugated peptide was labeled with the [$^{18}$F]AlF method with high radiochemical efficiency. Biodistribution and microPET imaging studies using tumor xenografted mice showed significant uptakes of the labeled peptide in $\alpha_v\beta_3$ integrin positive tumors. Blocking experiments demonstrated $\alpha_v\beta_3$ integrin specific uptake of the peptide. Synthesis of active ligand for general use and its application in labeling of peptides could facilitate further steps towards clinical applications of various labeled tracers.

## 4. Experimental section

### 4.1. General

$^{18}$F was produced by the medical cyclotron, CYCLONE® 18/9 (IBA, Louvain-la-Neuve, Belgium) by $^{18}$O (p, n) $^{18}$F nuclear reaction according to a standard procedure. 1,4-bis(*tert*-butoxycarbonylmethyl)-1,4,7-triazanonane (**1**) was synthesized according to previously reported method.[16] All other chemicals were purchased from Sigma/Aldrich (St. Louis, MO, U.S.A.). $^1$H and $^{13}$C NMR spectra were recorded on 300-MHz, AL-300 FTNMR spectrometer JEOL (Tokyo, Japan). Chemical shifts ($\delta$) were reported in ppm downfield from tetramethylsilane and Coupling constants are reported in hertz (Hz). The multiplicity is defined by s (singlet), d (doublet), t (triplet), dd (doublet of doublets), br (broad), and m (multiplet). $^1$H and $^{13}$C NMR spectra were acquired in $CDCl_3$ and reference to residual $CHCl_3$ at 7.26 and 77.00 ppm, respectively, or in $D_2O$ referenced to residual DOH at 4.65 ppm. Electrospray ionization mass spectra (ESI–MS) were acquired on a Waters ESI ion trap spectrometer (Milford, U.S.A.) for both positive and negative ion detection. The samples were diluted 1 to 100 with methanol and injected directly into the source. Data are reported in the form of (*m*/*z*) versus

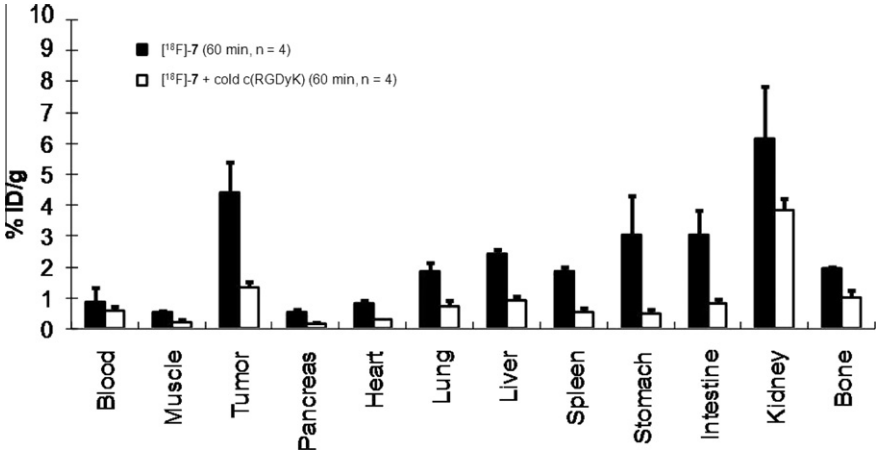


**Figure 3.** Biodistribution study (% D/g) of [$^{18}$F]7 directly injected and with co-injection of cold c(RGDyK) (3 mg/kg) in male BALB/c nude mice ($n$ = 8).

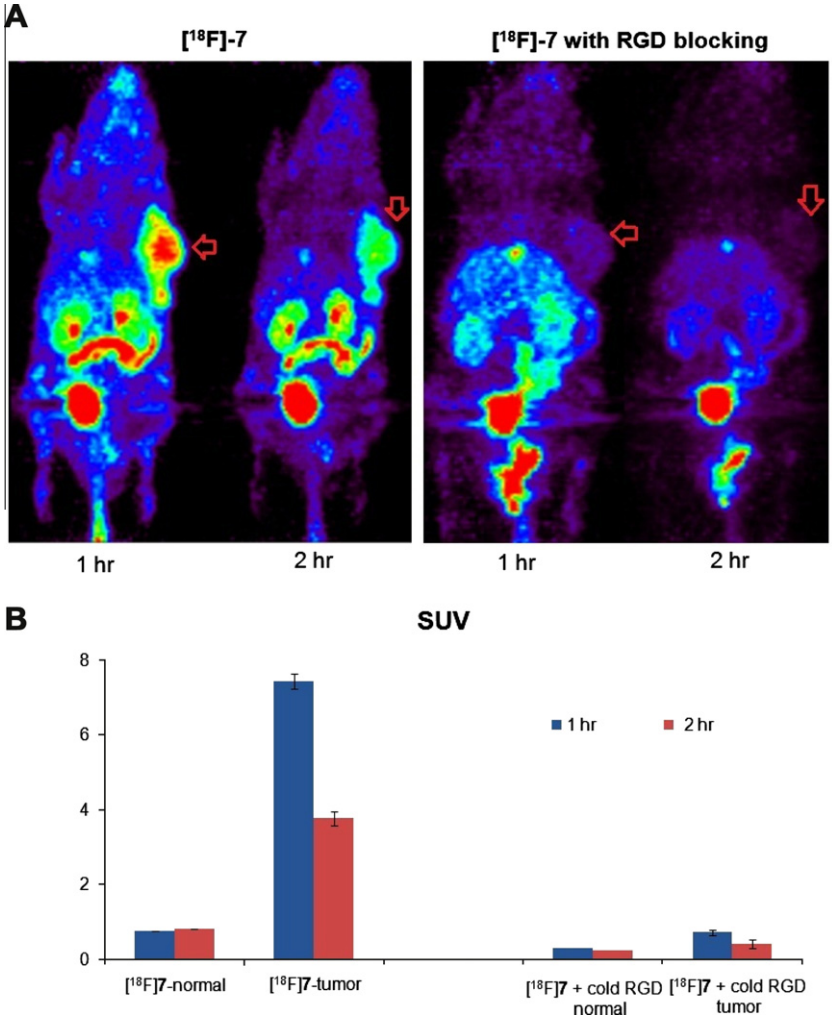


**Figure 4.** (A) Decay-corrected whole-body coronal microPET images of BALB/c nude mice bearing U87MG tumor and (B) SUVs of tumors and normal tissues (left shoulder) at 1 and 2 h post injection of [$^{18}$F]7 and [$^{18}$F]7 with c(RGDyK) as a blocking agent (3 mg/kg body weight). Arrows indicate tumors.

intensity. High resolution mass spectra were obtained on a Jeol, JMS-AX505WA, HP 5890 series II spectrometer using fast atomic bombardment ($FAB^+$) ionization detection.

Preparative HPLC purification of the compounds was performed on X-terra® 10 μm RP18 (19 × 250 mm) column. Analytical HPLC was performed on X-terra® 3.5 μm RP18 (4.6 × 100 mm) column. The solvent systems used were; solvent A (0.05% TFA solution in $H_2O$) and solvent B (EtOH). The flow rates were 1 mL/min for analytical HPLC and 7 mL/min for preparative HPLC, at the indicated linear gradients. Waters Sep-Pak Light Accell Plus QMA cartridge (Milford, U.S.A.) was used to obtain purified [$^{18}F^-$] solution. The gamma scintillation counter was a Packard Cobra II (GMI, MN,

U.S.A.). Radio-thin layer chromatography (TLC) was counted using a Bio-Scan AR-2000 System imaging scanner (Bioscan, DC, U.S.A.). Instant TLC-silica gel (ITLC–SG) plates were purchased from Varian Inc. (Agilent Technologies, Wilmington, U.S.A.). The biodistribution experiments were performed in Seoul National University Hospital, Seoul, Korea, which is fully accredited by AAALAC International (2007, Association for Assessment and Accreditation of Laboratory Animal Care International).

### 4.2. 4,7-Bis(tert-butoxycarbonylmethyl)-1-(4-nitro-benzyl)-1,4,7-triazanonane (2)

To a solution of **1** (0.2 g, 0.556 mmol) and $K_2CO_3$ (0.1 g, 0.556 mmol) in anhydrous acetonitrile (10 mL), 4-nitro benzyl bromide (0.12 g, 0.556 mmol) in acetonitrile (2 mL) was added slowly. Above reaction mixture was kept at room temperature with stirring for 20 h and monitored through thin layer chromatography (TLC, $CH_2Cl_2$/MeOH, 9/1, *v*/*v*). After completion, reaction mixture was filtered and solvent was evaporated. Crude product was purified by flash column chromatography ($CH_2Cl_2$/MeOH). Product, **2** was eluted in 7% of methanol. $^1$H NMR ($CDCl_3$, 300 MHz, 25 °C): $\delta$ 8.11–8.08 (d, 2H, $J$ = 9 Hz), 7.52–7.49 (d, 2H, $J$ = 9 Hz), 3.25 (s, 4H), 3.74 (s, 2H), 2.90–2.70 (m, 12H), 1.40 (s, 18H). $^{13}$C NMR ($CDCl_3$, 75 MHz, 25 °C): $\delta$ 171.3 (*C*O), 129.5, 123.5, 80.8, 61.7, 59.7, 55.5, 28.2. ESI-MS: $m/z$ = 493.3 for $[M+H]^+$.

### 4.3. 4,7-Bis(carboxymethyl)-1-(4-nitro-benzyl)-1,4,7-triazanonane (3)

Compound **2** (0.1 g, 0.204 mmol) was dissolved in 4 M HCl in 1,4-dioxane solution (8 mL) and kept for 24 h stirring at room temperature. Completion of the reaction was monitored by $ESI^+$ mass analysis. After the completion solvent was evaporated to obtain **3** as hydrochloride salt. $^1$H NMR ($D_2O$, 300 MHz, 25 °C): $\delta$ 8.06–8.03 (d, 2H, $J$ = 9 Hz), 7.58–7.55 (d, 2H, $J$ = 9 Hz), 4.37 (s, 2H), 3.58 (s, 4H), 3.50–3.30 (m, 6H), 3.15–2.90 (m, 6H). $^{13}$C NMR ($D_2O$, 75 MHz, 25 °C): $\delta$ 173.1 (*C*O), 149.0, 132.8, 124.8, 60.7, 56.7, 50.6, 49.8. ESI-MS: $m/z$ = 381.3 for $[M+H]^+$.

### 4.4. 4,7-Bis(carboxymethyl)-1-(4-amino-benzyl)-1,4,7-triazanonane (4)

Compound **3** (0.06 g, 0.156 mmol) was dissolved in 2 mM KOH solution in methanol (10 mL). Palladium on charcoal (Pd–C, 10%) was introduced to above solution under $N_2$. Above mixture was stirred under $H_2$ atmosphere for 8 h. Reaction mixture was filtered through celite and solvent was evaporated. Crude product was redissolved in water and purified by RP-HPLC (100% A for 5 min, 0 to 80% B for another 25 min). Eluted product peak ($t_R$ ~15 min) was evaporated completely to obtain product **4** as white solid. $^1$H NMR ($D_2O$, 300 MHz, 25 °C): $\delta$ 7.26–7.24 (d, 2H, $J$ = 6 Hz), 6.88–6.85 (d, 2H, $J$ = 9 Hz), 3.73 (s, 2H), 3.23 (s, 4H), 2.80–2.55 (m, 12H), 2.10 (s, 2H, –N*H*). $^{13}$C NMR ($D_2O$, 75 MHz, 25 °C): $\delta$ 180.4 (*C*O), 146.1, 131.8, 128.1, 122.7, 61.5, 60.5, 52.2, 51.2. ESI-MS: $m/z$ = 351.3 for $[M+H]^+$.

### 4.5. 4,7-Bis(carboxymethyl)-1-(4-isothiocyanato-benzyl)-1,4,7-triazanonane (5)

Thiophosgene (0.01 mL) was added dropwise into the mixture of **4** (0.04 g, 0.112 mmol), $CaCO_3$ (0.012 g, 0.172 mmol) and $H_2O$ (3 mL) in $CHCl_3$ (3 mL). The mixture was stirred overnight. After filtration, solvent was removed under vacuum and purified by RP-HPLC (100% A for 5 min, 0 to 100% B for another 25 min). Product peak was eluted at $t_R$ ~24 min. Collected fraction was evaporated to yield **5**. $^1$H NMR ($D_2O$, 300 MHz, 25 °C): $\delta$ 7.32–7.29 (d, 2H, $J$ = 9 Hz), 7.14–7.11 (d, 2H, $J$ = 9 Hz), 4.22 (s, 2H), 3.41 (s, 4H), 3.34–3.13 (m, 4H), 3.12–2.60 (m, 8H). $^{13}$C NMR ($D_2O$, 75 MHz, 25 °C): $\delta$ 174.2 (CO), 133.1, 132.7, 127.0, 60.1, 56.9, 50.9, 50.6, 49.2. ESI-MS: $m/z$ = 393.1 for $[M+H]^+$. HRMS ($FAB^+$) $m/z$ calcd for $C_{18}H_{24}N_4O_4S$ $[M+H]^+$ 393.1518, found 393.1524.

### 4.6. NODA-c(RGDyK) Conjugate (6)

A mixture of **5** (0.01 g, 0.026 mmol) and cRGDyK (0.016 g, 0.026 mmol) in 0.1 M sodium carbonate buffer (pH 9.5) was allowed to react for 15 h at room temperature. After completion of reaction, the reaction mixture was purified by RP-HPLC (100% A for 5 min, 0 to 100% B for another 25 min). Product peak was eluted at $t_R$ ~9.6 min. Collected product fraction was lyophilized after removing the EtOH to obtain product **6** as light yellow solid. $^1$H NMR ($D_2O$, 300 MHz, 25 °C): $\delta$ 7.87–7.84 (d, 2H, $J$ = 9 Hz), 7.66–7.63 (d, 2H, $J$ = 9 Hz), 7.34–7.31 (d, 2H, $J$ = 6 Hz), 7.01–6.98 (br s, 2H), 5.10–4.98 (m, 2H), 4.73 (s, 4H), 4.44–4.40 (d, 2H, $J$ = 12 Hz), 4.12–4.05 (br s, 2H), 3.89–2.95 (m, 24H), 2.45 (s, 2H), 2.32–1.12 (m, 16H). ESI-MS: $m/z$ = 1012.5 for $[M+H]^+$. HRMS ($FAB^+$) $m/z$ calcd for $C_{45}H_{65}N_{13}O_{12}S$ $[M+H]^+$ 1012.4596, found 1012.1524.

### 4.7. Radiolabeling experiment

Stock solution of 2 mM $AlCl_3$ was prepared by dissolving $AlCl_3{\cdot}6H_2O$ in 0.1 M sodium acetate buffer (pH 4). Sep-Pak Light Accell Plus QMA cartridge was pre-conditioned by eluting with 0.4 M $KHCO_3$ (5 mL), followed by water (10 mL). $^{18}F^-$ was loaded to the cartridge by eluting aqueous $^{18}F^-$ solution produced by a cyclotron and followed by washing with water (5 mL). The $^{18}F^-$ loaded cartridge was eluted with saline (0.4 mL) to obtain $^{18}F^-$ solution in saline. [$^{18}$F]AlF was prepared by mixing 45 nmol stock $AlCl_3$ (22.5 μL) and the eluted $^{18}F^-$ saline solutions (50 μL, 370 MBq). After adjusting pH to 4 by adding glacial acetic acid (4 μL), the mixture was incubated at room temperature for 10 min. The prepared [$^{18}$F]AlF solution (72.5 μL) was added to solution of **6** (50 nmol) in 0.1 M sodium acetate buffer (1 mL). Reaction mixture was heated to 110 °C on heating block for 10 min. The labeled compound was either purified by HPLC or passing through C-18 light cartridge to remove the unchelated [$^{18}$F]AlF resulted to obtain labeled peptide [$^{18}$F]AlF-NODA-RGD (**7**). Labeling efficiency was measured by ITLC–SG, eluted with 60% MeCN solution. Chromatography strips were monitored using a TLC scanner. Unlabeled [$^{18}$F]AlF remained at the origin and **7** moved to the solvent front. Stabilities in prepared medium at room temperature and in human serum at 37 °C were checked for 240 min. Extent of decomposition was checked by ITLC eluted with the same system above.

### 4.8. Biodistribution in U87MG xenografted BALB/c nude mice

Each BALB/c nude mouse was injected subcutaneously with $2 \times 10^5$/0.1 mL of U87MG (human glioma cells) cells in the right shoulder. After 11 days, labeled peptide [$^{18}$F]**7** (0.148 MBq/0.1 mL) was injected intravenously into each mouse through tail vein. For blocking studies, cold c(RGDyK) was injected (3 mg/kg body weight) along with labeled peptide. Mice were sacrificed 60 min post injection. Blood, muscle, bone and other organs were separated immediately and weighed. Counts were obtained with γ-scintillation counter. Percentages of injected dose per tissue weight (% ID/g) were calculated. Statistical analyses were performed by Student's t-test.

### 4.9. PET imaging in U87MG xenografted BALB/c nude mice

BALB/c mice bearing glioma xenografts were injected with [$^{18}$F]**7** (11.1 MBq/0.1 mL) through a tail vein. For inhibition exper-

iment, cold c(RGDyK) was injected (3 mg/kg body weight) along with labeled peptide. After inducing anesthesia with 2% isoflurane, PET images were obtained using a dedicated small animal PET/CT scanner (GE Healthcare, Princeton, NJ, USA). The acquired 3-dimensional emission data were reconstructed to temporally framed sinograms by Fourier rebinning using an ordered-subsets expectation maximization reconstruction algorithm without attenuation correction. ASIPro software (Concorde Microsystems Inc.) was used for image visualization.

## Acknowledgments

This research was supported partly by the National Research Laboratory Program of NRF (R0A-2008-000-20116-0) and the Converging Research Program funded by MEST (2010K001055).

## Supplementary data

Supplementary data associated with this article can be found, in the online version, at http://dx.doi.org/10.1016/j.bmc.2012.07.050.

## References and notes

[1]. Cai, W.; Zhang, X.; Wu, Y.; Chen, X. *J. Nucl. Med.* **2006**, *47*, 1172.
[2]. Chang, Y. S.; Jeong, J. M.; Lee, Y. S.; Kim, H. W.; Rai, G. B.; Lee, S. J.; Lee, D. S.; Chung, J. K.; Lee, M. C. *Bioconjug. Chem.* **2005**, *16*, 1329.
[3]. Lee, Y. S.; Jeong, J. M.; Kim, H. W.; Chang, Y. S.; Kim, Y. J.; Hong, M. K.; Rai, G. B.; Chi, D. Y.; Kang, W. J.; Kang, J. H.; Lee, D. S.; Chung, J. K.; Lee, M. C.; Suh, Y. G. *Nucl. Med. Biol.* **2006**, *33*, 677.
[4]. Poethko, T.; Schottelius, M.; Thumshirn, G.; Hersel, U.; Herz, M.; Henriksen, G.; Kessler, H.; Schwaiger, M.; Wester, H. J. *J. Nucl. Med.* **2004**, *45*, 892.
[5]. Wu, Z.; Li, Z. B.; Cai, W.; He, L.; Chin, F. T.; Li, F.; Chen, X. *Eur. J. Nucl. Med. Mol. Imaging* **1823**, *2007*, 34.
[6]. Laverman, P.; McBride, W. J.; Sharkey, R. M.; Eek, A.; Joosten, L.; Oyen, W. J.; Goldenberg, D. M.; Boerman, O. C. *J. Nucl. Med.* **2010**, *51*, 454.
[7]. McBride, W. J.; Sharkey, R. M.; Karacay, H.; D'Souza, C. A.; Rossi, E. A.; Laverman, P.; Chang, C. H.; Boerman, O. C.; Goldenberg, D. M. *J. Nucl. Med.* **2009**, *50*, 991.
[8]. Hoigebazar, L.; Jeong, J. M.; Choi, S. Y.; Choi, J. Y.; Shetty, D.; Lee, Y. S.; Lee, D. S.; Chung, J. K.; Lee, M. C.; Chung, Y. K. *J. Med. Chem.* **2010**, *53*, 6378.
[9]. Shetty, D.; Choi, S. Y.; Jeong, J. M.; Hoigebazar, L.; Lee, Y. S.; Lee, D. S.; Chung, J. K.; Lee, M. C.; Chung, Y. K. *Eur. J. Inorg. Chem.* **2010**, 5432.
[10]. Shetty, D.; Jeong, J. M.; Ju, C. H.; Kim, Y. J.; Lee, J. Y.; Lee, Y. S.; Lee, D. S.; Chung, J. K.; Lee, M. C. *Bioorg. Med. Chem.* **2010**, *18*, 7338.
[11]. Shetty, D.; Jeong, J. M.; Ju, C. H.; Lee, Y. S.; Jeong, S. Y.; Choi, J. Y.; Yang, B. Y.; Lee, D. S.; Chung, J. K.; Lee, M. C. *Nucl. Med. Biol.* **2010**, *37*, 893.
[12]. D'Souza, C. A.; McBride, W. J.; Sharkey, R. M.; Todaro, L. J.; Goldenberg, D. M. *Bioconjug. Chem.* **2011**, *22*, 1793.
[13]. Laverman, P.; D'Souza, C. A.; Eek, A.; McBride, W. J.; Sharkey, R. M.; Oyen, W. J.; Goldenberg, D. M.; Boerman, O. C. *Tumour Biol.* **2012**, *33*, 427.
[14]. McBride, W. J.; D'Souza, C. A.; Sharkey, R. M.; Goldenberg, D. M. *Appl. Radiat. Isot.* **2012**, *70*, 200.
[15]. McBride, W. J.; D'Souza, C. A.; Sharkey, R. M.; Karacay, H.; Rossi, E. A.; Chang, C. H.; Goldenberg, D. M. *Bioconjug. Chem.* **2010**, *21*, 1331.
[16]. Shetty, D.; Choi, S. Y.; Jeong, J. M.; Lee, J. Y.; Hoigebazar, L.; Lee, Y. S.; Lee, D. S.; Chung, J. K.; Lee, M. C.; Chung, Y. K. *Chem. Commun.* **2011**, *47*, 9732.
[17]. Hoigebazar, L.; Jeong, J. M.; Lee, J. Y.; Shetty, D.; Yang, B. Y.; Lee, Y. S.; Lee, D. S.; Chung, J. K.; Lee, M. C. *J. Med. Chem.* **2012**, *55*, 3155.
[18]. Feldser, D.; Agani, F.; Iyer, N. V.; Pak, B.; Ferreira, G.; Semenza, G. L. *Cancer Res.* **1999**, *59*, 3915.
[19]. Nishi, H.; Nakada, T.; Kyo, S.; Inoue, M.; Shay, J. W.; Isaka, K. *Mol. Cell. Biol.* **2004**, *24*, 6076.
[20]. Chiang, A. C.; Massague, J. *N. Eng. J. Med.* **2008**, *359*, 2814.
[21]. Klein, C. A. Cancer *Cancer Sci.* **2008**, *321*, 1785.
[22]. Podsypanina, K.; Du, Y. C. N.; Jechlinger, M.; Beverly, L. J.; Hambardzumyan, D.; Varmus, H. *Cancer Sci.* **1841**, *2008*, 321.
[23]. Bogler, O.; Mikkelsen, T. *Cancer J.* **2003**, *9*, 205.
[24]. Brooks, P. C.; Montgomery, A. M. P.; Rosenfeld, M.; Reisfeld, R. A.; Hu, T. H.; Klier, G.; Cheresh, D. A. *Cell* **1994**, *79*, 1157.
[25]. Folkman, J. *Semin. Oncol.* **2002**, *29*, 15.
[26]. Hood, J. D.; Cheresh, D. A. *Nat. Rev. Cancer* **2002**, *2*, 91.
[27]. Costouros, N. G.; Diehn, F. E.; Libutti, S. K. *J. Cell. Biochem.* **2002**, *87*, 72.
[28]. Haubner, R.; Beer, A. J.; Wang, H.; Chen, X. *Eur. J. Nucl. Med. Mol. Imaging* **2010**, *37*(Suppl 1), S86.
[29]. Haubner, R.; Wester, H. J. *Curr. Pharm. Des.* **2004**, *10*, 1439.
[30]. Jeong, J. M.; Hong, M. K.; Chang, Y. S.; Lee, Y. S.; Kim, Y. J.; Cheon, G. J.; Lee, D. S.; Chung, J. K.; Lee, M. C. *J. Nucl. Med.* **2008**, *49*, 830.
[31]. Beer, A. J.; Haubner, R.; Goebel, M.; Luderschmidt, S.; Spilker, M. E.; Wester, H. J.; Weber, W. A.; Schwaiger, M. *J. Nucl. Med.* **2005**, *46*, 1333.
[32]. Haubner, R.; Wester, H. J.; Burkhart, F.; Senekowitsch-Schmidtke, R.; Weber, W.; Goodman, S. L.; Kessler, H.; Schwaiger, M. *J. Nucl. Med.* **2001**, *42*, 326.
[33]. Haubner, R.; Wester, H. J.; Weber, W. A.; Mang, C.; Ziegler, S. I.; Goodman, S. L.; Senekowitsch-Schmidtke, R.; Kessler, H. *Cancer Res.* **2001**, *61*, 1781.
[34]. Kenny, L. M.; Coombes, R. C.; Oulie, I.; Contractor, K. B.; Miller, M.; Spinks, T. J.; McParland, B.; Cohen, P. S.; Hui, A. M.; Palmieri, C.; Osman, S.; Glaser, M.; Turton, D.; Al-Nahhas, A.; Aboagye, E. O. *J. Nucl. Med.* **2008**, *49*, 879.
[35]. McParland, B. J.; Miller, M. P.; Spinks, T. J.; Kenny, L. M.; Osman, S.; Khela, M. K.; Aboagye, E.; Coombes, R. C.; Hui, A. M.; Cohen, P. S. *J. Nucl. Med.* **2008**, *49*, 1664.
[36]. Morrison, M. S.; Ricketts, S. A.; Barnett, J.; Cuthbertson, A.; Tessier, J.; Wedge, S. R. *J. Nucl. Med.* **2009**, *50*, 116.
[37]. Kim, H. W.; Jeong, J. M.; Lee, Y. S.; Chi, D. Y.; Chung, K. H.; Lee, D. S.; Chung, J. K.; Lee, M. C. *Appl. Radiat. Isot.* **2004**, *61*, 1241.
[38]. Lang, L.; Li, W.; Guo, N.; Ma, Y.; Zhu, L.; Kiesewetter, D. O.; Shen, B.; Niu, G.; Chen, X. *Bioconjug. Chem.* **2011**, *22*, 2415.
[39]. Liu, S.; Liu, H.; Jiang, H.; Xu, Y.; Zhang, H.; Cheng, Z. *Eur. J. Nucl. Med. Mol. Imaging* **2011**, 1.